Redefining Forme Fruste Keratoconus

Marcella Quaresma Salomão, Ana Luisa Höffling-Lima, Louise Pellegrino Gomes Esporcatte, Fernando Faria Correia, Bernardo T. Lopes, Nelson Sena Jr., Aydano Pamponet Machado, and Renato Ambrósio Jr.

1 Introduction

Over 150 years ago, John Nottingham, in England, presented the first endorsed medical publication associated with keratoconus (KC) and ectatic corneal diseases [1]. Since then, KC has been widely investigated throughout the decades, but it was the advent of refractive surgery in the 1990s that boosted research on ectatic corneal diseases. This fact is associated with the need to identify not only milder forms of ectatic disease but also eyes that are vulnerable to biomechanical decompensation

M. Q. Salomão (✉)
Instituto de Olhos Renato Ambrósio, Rio de Janeiro, RJ, Brazil

Rio de Janeiro Corneal Tomography and Biomechanics Study Group, Rio de Janeiro, RJ, Brazil

Brazilian Study Group of Artificial Intelligence and Corneal Analysis (BrAIN), Rio de Janeiro, RJ, Brazil/Maceió, AL, Brazil

Department of Ophthalmology, Federal University of São Paulo, São Paulo, SP, Brazil

Instituto Benjamin Constant, Rio de Janeiro, RJ, Brazil
e-mail: marcella@barravisioncenter.com.br

A. L. Höffling-Lima
Department of Ophthalmology, Federal University of São Paulo, São Paulo, SP, Brazil

L. P. G. Esporcatte
Rio de Janeiro Corneal Tomography and Biomechanics Study Group, Rio de Janeiro, RJ, Brazil

Instituto de Olhos Renato Ambrósio, Rio de Janeiro, RJ, Brazil

Department of Ophthalmology, Federal University of São Paulo, São Paulo, SP, Brazil

F. Faria Correia
Braga Hospital, Braga, Portugal

School of Medicine, University of Minho, Braga, Portugal

E. Almodin et al. (eds.), *Keratoconus*,
https://doi.org/10.1007/978-3-030-85361-7_72

and further iatrogenic ectasia after laser vision correction (LVC) [2–6]. Additionally, the emergence of new treatment modalities—such as corneal collagen cross-linking (CXL), customized surface ablation, intrastromal corneal ring segments, and phakic intraocular lenses—has encouraged developments in this field, as these techniques equally benefit from early diagnosis [7–11].

KC is a bilateral and habitually asymmetric ectatic corneal disease associated with chronic biomechanical decompensation and subsequent corneal protrusion, causing irregular astigmatism and impacting visual acuity [12, 13]. The presentation and progression of this disease can vary greatly between patients, and different terminologies have been applied to different presentations.

2 Terminology for Ectatic Corneal Diseases: Forme Fruste

The term *fruste* is derived from French. It means "crude or unfinished" and has been classically used to specify an incomplete form of a disease. It is used in several fields of medicine in order to describe an atypical or attenuated manifestation of a disease or syndrome. The opposite situation is known as *forme plaine*, which means the complete or "full-blown" form of a disease. Conceptually, a forme fruste of any disease might progress (or not) to a forme plaine, depending on several factors.

B. T. Lopes
Renato Ambrósio Eye Institute, Rio de Janeiro, RJ, Brazil

Rio de Janeiro Corneal Tomography and Biomechanics Study Group, Rio de Janeiro, RJ, Brazil

Department of Ophthalmology, Federal University of São Paulo, São Paulo, SP, Brazil

School of Engineering, University of Liverpool, Liverpool, UK

N. Sena Jr.
Department of Ophthalmology, Federal University of the State of Rio de Janeiro, Rio de Janeiro, RJ, Brazil

A. P. Machado
Brazilian Study Group of Artificial Intelligence and Corneal Analysis (BrAIN), Rio de Janeiro, RJ, Brazil/Maceió, AL, Brazil

Department of Ophthalmology, Federal University of São Paulo, São Paulo, SP, Brazil

Computing Institute, Federal University of Alagoas, Maceió, AL, Brazil

R. Ambrósio Jr.
Rio de Janeiro Corneal Tomography and Biomechanics Study Group, Rio de Janeiro, RJ, Brazil

Instituto de Olhos Renato Ambrósio, Rio de Janeiro, RJ, Brazil

Department of Ophthalmology, Federal University of São Paulo, São Paulo, SP, Brazil

Brazilian Study Group of Artificial Intelligence and Corneal Snalysis (BrAIN), Rio de Janeiro, RJ, Brazil/Maceió, AL, Brazil

Department of Ophthalmology, Federal University of the State of Rio de Janeiro, Rio de Janeiro, RJ, Brazil

Decades before the advent of computerized corneal topography and refractive surgery, Marc Amsler, back in 1938, was the first person to describe forme fruste keratoconus (FFKC). Amsler used Plácido disk photokeratoscopy in order to prospectively evaluate contralateral eyes of patients with known KC that did not present any slit lamp signs or Plácido imaging abnormalities [14, 15]. Different situations have been described as FFKC, including the normal topographic eye in very asymmetric ectasia (VAE) cases or even a normal topographic eye that naturally evolves clinical ectasia during longitudinal follow-up [16]. Terms such as *subclinical* or *incomplete* have also been applied and interchangeably used to describe such cases. It is important to mention that very mild KC might occur in both eyes of the same patient, and this is described as bilateral FFKC. *Keratoconus suspect* (KCS) is another term that has been coined to describe an abnormal topographic pattern that does not yet fulfill the criteria for KC. These cases may truly be mild forms of KC or may eventually present stable topographic and biomechanical behavior and even become good candidates for successful laser vision correction [16–21].

Several clinical biomicroscopic signs of KC have been described in the literature, including enlargement of corneal nerves, Vogt's striae, Munson's sign, Ruzzuti's sign, and Fleisher rings [22]. These are typically late signs of the disease, which can be promptly identified by a trained physician. However, the critical need for earlier diagnosis (before the appearance of these signs) and identification of milder forms of the disease became evident with Seiler's seminal publication on progressive iatrogenic ectasia after laser vision correction in an eye with FFKC [2]. Thus, there is a fundamental need for enhanced sensitivity to identify such cases. The latest developments in multimodal imaging with high-resolution techniques have been shown to increase the overall accuracy of early disease detection. Moreover, the association and integration of artificial intelligence strategies is an extremely promising approach and has so far demonstrated an additive effect, augmenting our ability to diagnose mild KC cases [23].

3 Diagnostic Tools

3.1 Corneal Topography

In the late 1980s, computerized corneal topography was introduced [24], and huge efforts to develop this technology have been made since then. Plácido disk–based corneal topography represents quantitative anterior surface data through color-coded maps [25]. Rabinowitz and McDonnell proposed topographic indices—such as inferior–superior asymmetry, between-eyes asymmetry, and central corneal power—to detect KC [26]. These indices are still applied for topographic diagnosis of KC and have proved to be sensitive in identifying milder ectatic patterns as well [27, 28]. Interestingly, Rabinowitz describes eyes with FFKC as eyes that have unremarkable biomicroscopy, no visual impairment, and good corrected distance visual acuity (CDVA) with glasses but present typical keratoconus irregularity on topographic mapping. Randleman and coworkers combined corneal topography,

corneal pachymetry, and clinical data to develop the ectasia risk score system, considering FFKC a topographic classification with a major risk of ectasia after laser-assisted in situ keratomileusis (LASIK) [29, 30]. This is in agreement with a seminal report by Seiler of iatrogenic keratectasia after LASIK in a case of forme fruste keratoconus [2]. However, the limitations of this approach were realized after disclosure of cases that developed post–refractive surgery ectasia despite normal anterior curvature maps [31–33], along with eyes with abnormal preoperative topographic maps that underwent laser vision correction and presented documented stability based on advanced corneal imaging [21]. Furthermore, the subjective classification of these topographic maps represents an important limitation in itself. Studies have demonstrated major variability among experts and even with the same examiner using different color-coded scales [34].

3.2 Corneal Tomography

Corneal tomography evolved into more complete corneal analysis with corneal tomography [35, 36]. This approach provides a three-dimensional reconstruction of the cornea with measurements of both anterior and posterior corneal surfaces. Different systems—including slit scanning, rotational Scheimpflug imaging, very high-frequency ultrasound, and optical coherence tomography (OCT)—allow this approach.

The Orbscan (Bausch + Lomb, Rochester, NY, USA) was the first instrument introduced into the market. Reports have demonstrated good sensitivity and specificity of Orbscan indices to detect early forms of KC, even in cases with innocent Plácido disk–based topography [37]. More recently, special software developed using linear regression analysis was designed for the Orbscan, to objectively classify topographic maps as positive or negative for ectasia risk. The Screening Corneal Objective Risk of Ectasia (SCORE) analyzer has been tested and validated in FFKC cases and post-LASIK ectasia cases as well [38–40].

The Galilei dual-Scheimpflug analyzer (Ziemer Ophthalmic Systems, Port, Switzerland) is a system that unites Scheimpflug imaging with Plácido disk–based corneal topography. Investigators have demonstrated the ability of this technique not only to discriminate between normal and KC eyes [41] but also to detect abnormalities in topographically normal fellow eyes of patients with very asymmetric ectasia [42, 43]. Pentacam (Oculus, Wetzlar, Germany) was the first rotating Scheimpflug system available, and several indices have been proposed to improve the diagnosis of KC using this device. One of the main displays available for preoperative screening is the Pentacam Belin/Ambrósio enhanced ectasia display (BAD) deviation index (BAD-D). This clinical tool combines pachymetric and elevation data in order to assist KC diagnosis. Tomographic parameters are displayed as standard deviations from normality (d values), and linear regression analysis applies different weights to each parameter and calculates a final D value [44, 45]. Studies involving normal and keratoconic eyes have found high sensitivity and specificity values using this approach [35]. Studies involving highly asymmetric cases have

also been conducted, and the ability of this method to detect abnormalities in these cases has been evidenced as well [35]. Finally, retrospective studies involving eyes that developed ectasia after LASIK have also been performed, and researchers found higher accuracy of this technology in order to identify susceptible cases, these cases have already been considered good candidates for lasik, based on corneal topography [46, 47].

Machine learning algorithms and artificial intelligence (AI) methods have been effectively used to combine Pentacam parameters. The Pentacam random forest index (PRFI) was developed in a study that analyzed preoperative data from groups of normal eyes, eyes with clinical keratoconus, topographically normal eyes in patients with very asymmetric ectasia, and eyes with ectasia susceptibility (in patients who developed post-LASIK ectasia) [48]. The PRFI demonstrated high performance in discriminating between the four groups. Ambrósio and coworkers applied logistic regression analysis to investigate the benefit of integrating clinical and tomographic data to discriminate between eyes that remained stable after lasik and eyes that developed iatrogenic ectasia after LASIK. This retrospective analysis demonstrated higher sensitivity and specificity with the combination of parameters than with the individual parameters alone in identifying preoperative ectasia susceptibility [49].

3.3 Segmental or Layered Tomography

Characterization of the individual corneal layers was the next step in corneal tomography evolution. Reinstein and collaborators pioneered corneal epithelial measurements with very high-frequency ultrasound (VHF-US) [50]. The role of corneal epithelial measurements has been evidenced in several clinical situations in the refractive surgery field [51]. Corneal epithelial indices derived from VHF-US have also been proposed as a valuable tool for detecting KC, even in milder forms of the disease [52, 53].

Huang and collaborators developed a parallel approach with OCT. These authors explored an extended epithelial thickness map, which, along with different epithelial indices, was able to detect KC, even in milder stages [54, 55].

Additionally, Sinha-Roy and coauthors developed a new Bowman's roughness index derived from OCT technology. These authors compared the level of irregularity of the Bowman's layer in healthy and keratoconic eyes and found significant differences between them. The authors demonstrated even higher sensitivity in identifying mild forms of KC when this index was combined with epithelial thickness data and the BAD-D value [56].

3.4 Corneal Biomechanical Assessment

There is a major consensus that ectatic corneal diseases are related to abnormal biomechanical properties and that a focal biomechanical abnormality starts the process that ends up as secondary thinning and deformation [57]. Thus,

characterization of the cornea beyond its shape may be critical for enhancing the accuracy of ectatic disease identification, especially in early stages.

The Ocular Response Analyzer (ORA; Reichert Ophthalmic Instruments, Depew, NY, USA) was the first commercially available instrument to measure corneal biomechanical properties [58]. This noncontact tonometer generates two main biomechanical parameters: corneal hysteresis (CH) and the corneal resistance factor (CRF). Studies have demonstrated that although CH and the CRF have significantly different distributions in healthy and ectatic eyes, the use of this technology in KC diagnosis is limited because a significant overlap has been found in the comparisons [59]. New parameters derived from wave form signals and also combination of tomographic and biomechanical parameters using logistic regression analysis have demonstrated higher accuracy in discriminating between normal and ectatic eyes [60–63].

The Corvis ST (Oculus Optikgeräte, Wetzlar, Germany) is another noncontact tonometer equipped with an ultra high-speed Scheimpflug camera, which examines the whole corneal deformation process. The device provides a set of deformation parameters, including the deformation amplitude, the radius of curvature at the highest concavity, applanation lengths, and corneal velocities [64, 65]. As with the ORA, despite significant differences, a substantial overlap was evidenced in comparisons of normal and KC eyes [66, 67].

Nevertheless, the combination of deformation parameters with AI techniques has enhanced the accuracy of discrimination between normal and keratoconic corneas, even in early stages [65].

More recently, a new Corvis ST biomechanical parameter—the Corvis biomechanical index (CBI)—was introduced to characterize ectatic corneas. Linear regression analysis was employed to combine horizontal thickness profile data with corneal deformation parameters. A cut off of 0.5 provided values of 94.1% sensitivity and 100% specificity in the training database [68] and 98.4% specificity and 100% sensitivity in the validation study [68].

Subsequently, Ambrósio and collaborators continued to apply AI methods to further augment the ability to detect ectatic diseases. These authors introduced the tomographic and biomechanical index (TBI), which combines Scheimpflug-based tomographic data and biomechanical data [5]. The first cut off of 0.79 demonstrated high sensitivity and specificity values when discriminating between normal and frank ectatic eyes. Later, an optimized cut off value of 0.29 provided 90.4% sensitivity and 96% specificity. Subsequent validation studies confirmed the capacity of the TBI to identify corneal ectasia [69].

3.5 Ocular Wave Front Analysis

Ocular aberrometry is a diagnostic tool applied in investigation of ocular aberrations, especially for planning wave front–guided refractive surgery [70]. Investigation of higher-order aberrations has proven to be valuable in different corneal disorders as well, including KC [71]. Comparative studies have demonstrated that corneal and total higher-order aberrations are significantly more severe in KC eyes than in

healthy eyes [72, 73]. Interestingly, the ocular wave front has proven to be valuable in the detection of milder forms of KC as well [74, 75].

4 Clinical Examples

4.1 Case 1: Very Asymmetric Ectasia with Forme Fruste Keratoconus

A 27-year-old male patient sought a second opinion after diagnosis of "unilateral" KC. His uncorrected distance visual acuity (UDVA) 20/20 in his right eye (OD) and 20/800 in his left eye (OS), which did not improve with spectacles or contact lenses. Figure 1 demonstrates Pentacam axial corneal topography, along with OD pachymetric and elevation maps. KC topometric patterns were not detected in this eye, whereas the contralateral eye demonstrated advanced KC (Fig. 2). Tomographic and biomechanical integration demonstrated abnormal BAD-D and TBI values in the right eye despite an innocent topographic map (Fig. 3). This anecdotal example demonstrates a case of very asymmetric ectasia with FFKC in OD that could be diagnosed only with multimodal corneal imaging and integration of different approaches with artificial intelligence.

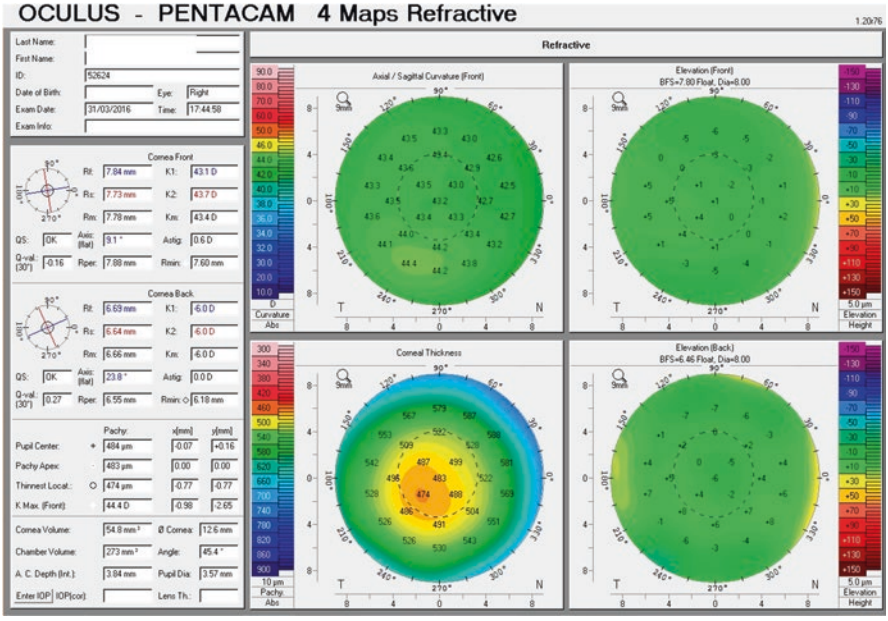

Fig. 1 Case 1: Pentacam quad map showing anterior corneal curvature, pachymetry, and elevation data from the right eye. Note the relatively innocent topographic map and the absence of abnormalities on the pachymetry and elevation maps

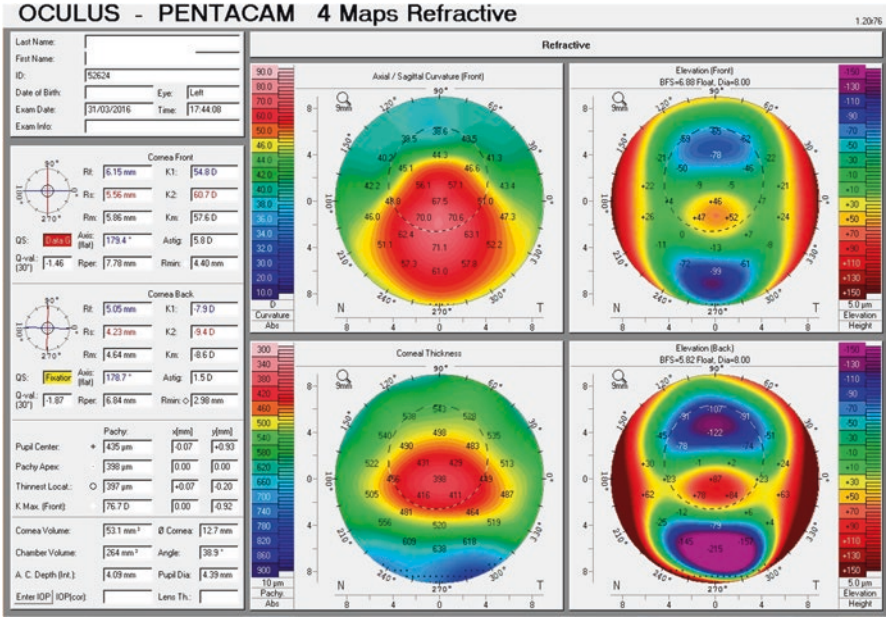

Fig. 2 Case 1: Pentacam quad map of the left eye. Note the advanced keratoconus stage, with typical abnormalities in the pachymetry and elevation evaluations

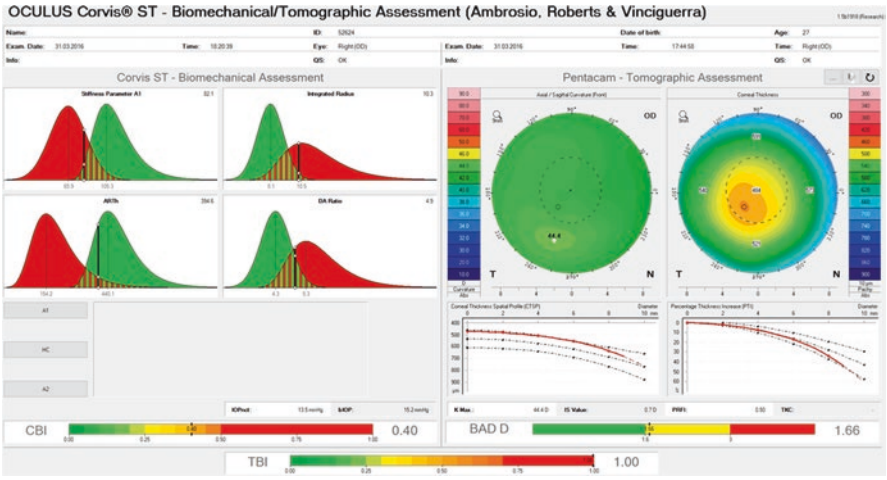

Fig. 3 Case 1: Corvis ST tomographic–biomechanical display of the right eye (OD). Note the abnormal tomographic and biomechanical index (TBI) value of 1.00, despite the relatively normal topographic map. *BAD-D* Belin/Ambrósio enhanced ectasia display (BAD) deviation index, *CBI* Corvis biomechanical index

4.2 Case 2: Unilateral Ectasia

In this case of a 39-year-old male patient referred for specialized KC treatment in the right eye, the UDVA was 20/60 in the right eye and 20/30 in the left eye. The manifest refraction was −1.75 −4.00 × 35° in the right eye and −0.50 −0.25 × 115° in the left eye. The corrected distance visual acuity (CDVA) was 20/40 in the right eye and 20/15 in the left eye. Plácido disk–based corneal topography obtained using Keratograph 5 (Oculus, Wetzlar, Germany) demonstrated a marked irregularity with a truncated bow tie in OD but relatively normal asphericity and low astigmatism in OS. The Oculus topometric keratoconus classification (TKC) was consistent with grade 2 keratoconus in the right eye and had no similarity to the ectatic disease in the left eye (Fig. 4). Tomographic and biomechanical evaluation demonstrated absolutely normal CBI, BAD-D, and TBI values (Fig. 5). Interestingly, further evaluation with segmental tomography by spectral domain OCT was possible, and no abnormalities corresponding to KC were found. This example demonstrates very asymmetric ectasia with unilateral ectasia. This is in agreement with the consensus

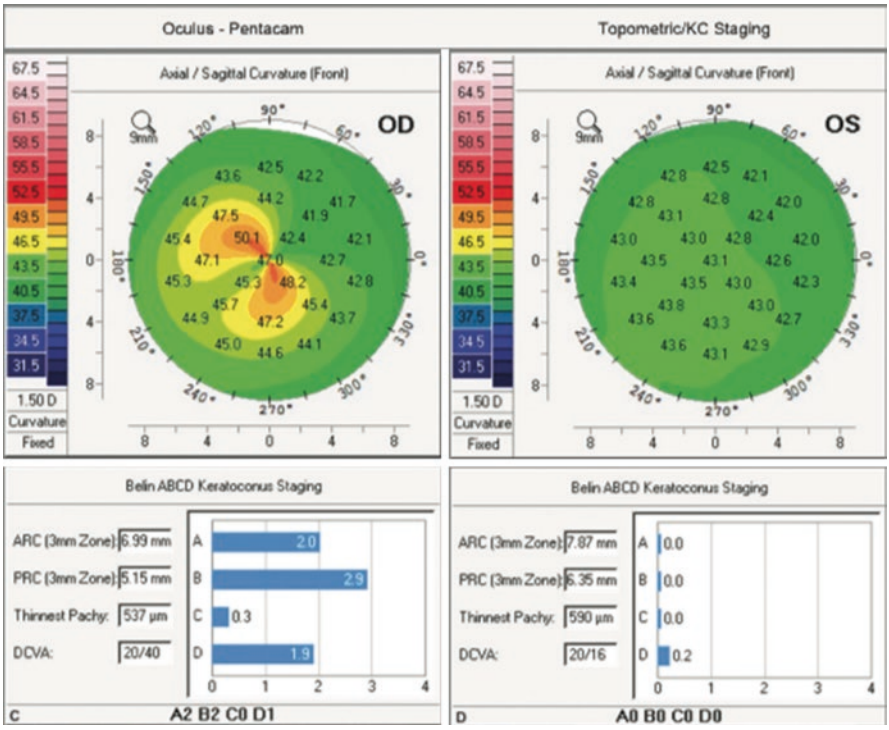

Fig. 4 Case 2: Keratograph 5 front surface axial curvature (topometric) maps, including Belin ABCD keratoconus staging. Note the steep and truncated bow tie in the right eye (OD) and the low asphericity and astigmatism in the left eye (OS). The Oculus topometric keratoconus classification demonstrated grade 2 keratoconus in the right eye, which had no similarity to the ectatic disease in the left eye

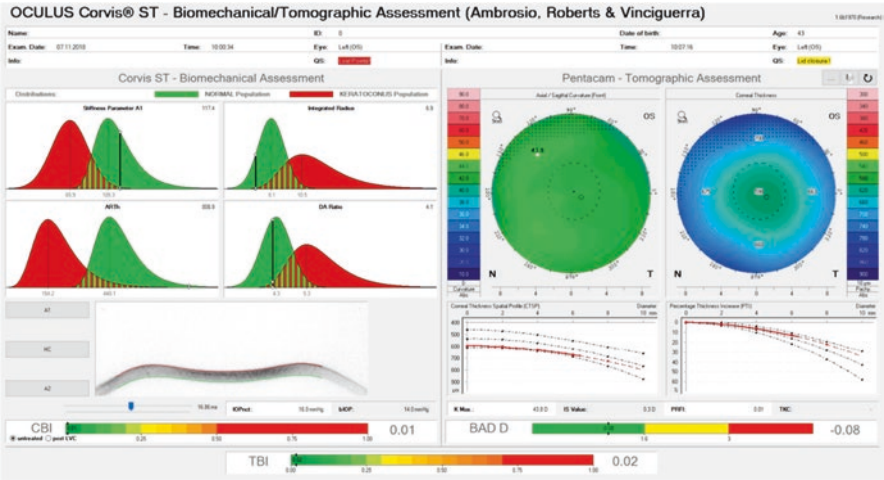

Fig. 5 Case 2: Corvis ST tomographic–biomechanical display of the left eye (OS). Note the normal Corvis biomechanical index (CBI) value (0.01), Belin/Ambrósio enhanced ectasia display (BAD) deviation index (BAD-D) value (−0.08), and tomographic and biomechanical index (TBI) value (0.02)

that true unilateral KC does not exist but secondary ectasia might occur unilaterally. Studies with longitudinal data should be performed to test this concept.

4.3 Case 3: Bilateral Forme Fruste Keratoconus

This is an anecdotal example of an 11-year-old boy whose mother developed ectasia after LASIK in OS. The boy's visual acuity was 20/20 in both eyes (OU), and he had a normal slit lamp examination, except for moderate allergy findings. Curiously, tomographic and biomechanical evaluation demonstrated abnormal CBI and TBI findings in both eyes, despite a relatively normal anterior curvature map in OU (Figs. 6 and 7). This example is a case of bilateral FFKC, where very mild KC occurs in both eyes of the same patient. Interestingly, the family history was positive for ectasia, which emphasizes the need for genetic testing.

5 Conclusion

The description of forme fruste keratoconus (FFKC) started with Amsler, many decades ago [14, 15]. In 2009, Klyce suggested that the term FFKC should be applied only to the contralateral eye of KC patients with normal topography and no other clinical features of ectasia [16] and that accordingly, the term KCS should be applied only to corneas with topographic abnormalities that are not yet definitive of KC [16]. The global consensus is that although KC may present with a high degree

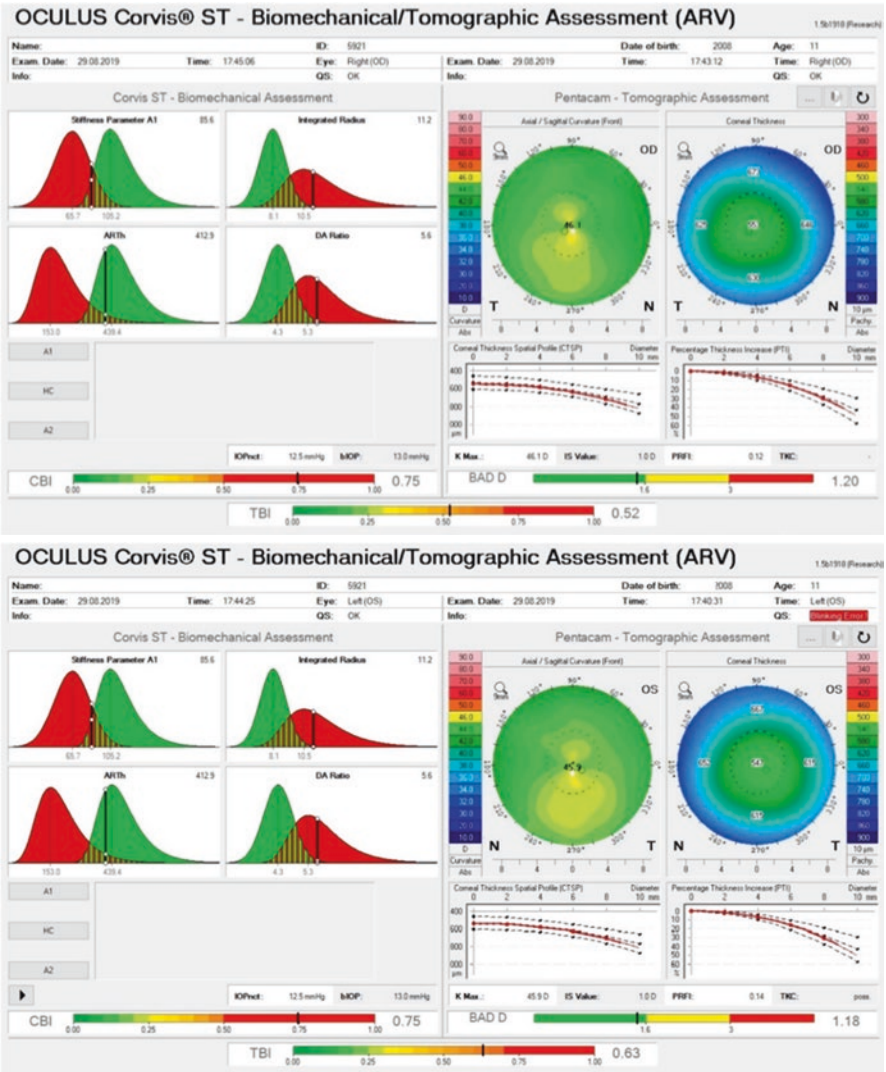

Figs. 6 and 7 Case 3: Corvis ST tomographic–biomechanical display of both eyes. Note that despite relatively normal anterior curvature maps, the Corvis biomechanical index (CBI) values were abnormal (0.75 in both eyes) as were the tomographic and biomechanical index (TBI) values (0.52 in the right eye [OD] and 0.63 in the left eye [OS]). *BAD-D* Belin/Ambrósio enhanced ectasia display (BAD) deviation index

of asymmetry, the disease is typically bilateral [57]. However, there is also agreement that unilateral ectasia secondary to an iatrogenic biomechanical process may occur. In this case, the term *unilateral ectasia*, and not the term *keratoconus*, should be applied. Interestingly, studies have documented cases of unilateral ectasia with long-term stability tracked by advanced diagnostic methods [76, 77].

Interestingly, very recently, Henriquez and coworkers performed a systematic literature review on KCS and FFKC, concluding that there is a significant lack of unified criteria to define these cases [78].

The redefinition of FFKC is intrinsically associated with refractive surgery and KC management. FFKC is not a topographic or even a tomographic classification and should be defined as very high susceptibility to ectasia progression. Screening for ectasia risk among refractive candidates goes beyond disease diagnosis into understanding inherent susceptibility. Advances in corneal imaging with a multimodal approach allow for improvements in sensitivity and specificity to identify this susceptibility.

References

1. Gokul A, Patel DV, McGhee CN. Dr John Nottingham's 1854 landmark treatise on conical cornea considered in the context of the current knowledge of keratoconus. Cornea. 2016;35:673–8.
2. Seiler T, Quurke AW. Iatrogenic keratectasia after LASIK in a case of forme fruste keratoconus. J Cataract Refract Surg. 1998;24:1007–9.
3. Binder PS, Lindstrom RL, Stulting RD, et al. Keratoconus and corneal ectasia after LASIK. J Cataract Refract Surg. 2005;31:2035–8.
4. Ambrósio R Jr, Randleman JB. Screening for ectasia risk: what are we screening for and how should we screen for it? J Refract Surg. 2013;29:230–2.
5. Ambrósio R Jr, Lopes BT, Faria-Correia F, et al. Integration of Scheimpflug-based corneal tomography and biomechanical assessments for enhancing ectasia detection. J Refract Surg. 2017;33:434–43.
6. Ambrósio R. Post-LASIK ectasia: twenty years of a conundrum. Semin Ophthalmol. 2019;34:66–8.
7. Ambrósio R Jr, Faria-Correia F, Silva-Lopes I, Azevedo-Wagner A, Tanos FW, Lopes B, Salomão M. Paradigms, paradoxes and controversies on keratoconus and corneal ectatic diseases. Int J Keratoconus Ectatic Corneal Dis. 2018;7:35–49.
8. Ambrósio R Jr, Lopes B, Amaral J, et al. Ceratocone: quebra de paradigmas e contradições de uma nova subespecialidade. Rev Bras Oftalmol. 2019;78:81–5.
9. McGhee CN, Kim BZ, Wilson PJ. Contemporary treatment paradigms in keratoconus. Cornea. 2015;34(Suppl 10):S16–23.
10. Belin MW, Duncan JK. Keratoconus: the ABCD grading system. Klin Monatsbl Augenheilkd. 2016;233:701–7.
11. Duncan JK, Belin MW, Borgstrom M. Assessing progression of keratoconus: novel tomographic determinants. Eye Vis (Lond). 2016;3:6.
12. Rabinowitz YS. Keratoconus. Surv Ophthalmol. 1998;42:297–319.
13. Krachmer JH, Feder RS, Belin MW. Keratoconus and related noninflammatory corneal thinning disorders. Surv Ophthalmol. 1984;28:293–322.
14. Amsler M. Some data on the problem of keratoconus [in French]. Bull Soc Belge Ophtalmol. 1961;129:331–54.
15. Amsler M. Classic keratocene and crude keratocene; unitary arguments [in French]. Ophthalmologica. 1946;111:96–101.
16. Klyce SD. Chasing the suspect: keratoconus. Br J Ophthalmol. 2009;93:845–7.
17. Ambrósio R Jr, Klyce SD, Wilson SE. Corneal topographic and pachymetric screening of keratorefractive patients. J Refract Surg. 2003;19:24–9.
18. Maeda N, Klyce SD, Tano Y. Detection and classification of mild irregular astigmatism in patients with good visual acuity. Surv Ophthalmol. 1998;43:53–8.

19. Smolek MK, Klyce SD. Goodness-of-prediction of Zernike polynomial fitting to corneal surfaces. J Cataract Refract Surg. 2005;31:2350–5.
20. Smolek MK, Klyce SD, Maeda N. Keratoconus and contact lens–induced corneal warpage analysis using the keratomorphic diagram. Invest Ophthalmol Vis Sci. 1994;35:4192–204.
21. Reinstein DZ, Archer TJ, Gobbe M. Stability of LASIK in topographically suspect keratoconus confirmed non-keratoconic by Artemis VHF digital ultrasound epithelial thickness mapping: 1-year follow-up. J Refract Surg. 2009;25:569–77.
22. Zadnik K, Barr JT, Gordon MO, Edrington TB. Biomicroscopic signs and disease severity in keratoconus. Collaborative Longitudinal Evaluation of Keratoconus (CLEK) Study Group. Cornea. 1996;15:139–46.
23. Lopes BT, Ramos IC, Salomão MQ, et al. Enhanced tomographic assessment to detect corneal ectasia based on artificial intelligence. Am J Ophthalmol. 2018;195:223–32.
24. Klyce SD, Wilson SE, Kaufman HE. Corneal topography comes of age. Refract Corneal Surg. 1989;5:359–61.
25. Wilson SE, Ambrósio R. Computerized corneal topography and its importance to wavefront technology. Cornea. 2001;20:441–54.
26. Rabinowitz YS, McDonnell PJ. Computer-assisted corneal topography in keratoconus. Refract Corneal Surg. 1989;5:400–8.
27. Maeda N, Klyce SD, Smolek MK, Thompson HW. Automated keratoconus screening with corneal topography analysis. Invest Ophthalmol Vis Sci. 1994;35:2749–57.
28. Maguire LJ, Bourne WM. Corneal topography of early keratoconus. Am J Ophthalmol. 1989;108:107–12.
29. Randleman JB, Woodward M, Lynn MJ, Stulting RD. Risk assessment for ectasia after corneal refractive surgery. Ophthalmology. 2008;115:37–50.
30. Randleman JB, Trattler WB, Stulting RD. Validation of the ectasia risk score system for preoperative laser in situ keratomileusis screening. Am J Ophthalmol. 2008;145:813–8.
31. Klein SR, Epstein RJ, Randleman JB, Stulting RD. Corneal ectasia after laser in situ keratomileusis in patients without apparent preoperative risk factors. Cornea. 2006;25:388–403.
32. Ambrósio R Jr, Dawson DG, Salomão M, Guerra FP, Caiado AL, Belin MW. Corneal ectasia after LASIK despite low preoperative risk: tomographic and biomechanical findings in the unoperated, stable, fellow eye. J Refract Surg. 2010;26:906–11.
33. Malecaze F, Coullet J, Calvas P, Fournié P, Arné JL, Brodaty C. Corneal ectasia after photorefractive keratectomy for low myopia. Ophthalmology. 2006;113:742–6.
34. Ramos IC, Correa R, Guerra FP, et al. Variability of subjective classifications of corneal topography maps from LASIK candidates. J Refract Surg. 2013;29:770–5.
35. Ambrósio R Jr, Valbon BF, Faria-Correia F, Ramos I, Luz A. Scheimpflug imaging for laser refractive surgery. Curr Opin Ophthalmol. 2013;24:310–20.
36. Ambrósio R Jr, Belin MW. Imaging of the cornea: topography vs tomography. J Refract Surg. 2010;26:847–9.
37. Saad A, Gatinel D. Topographic and tomographic properties of forme fruste keratoconus corneas. Invest Ophthalmol Vis Sci. 2010;51:5546–55.
38. Chan C, Ang M, Saad A, et al. Validation of an objective scoring system for forme fruste keratoconus detection and post-LASIK ectasia risk assessment in Asian eyes. Cornea. 2015;34:996–1004.
39. Saad A, Gatinel D. Validation of a new scoring system for the detection of early forme of keratoconus. Int J Keratoconus Ectatic Corneal Dis. 2012;1:100–8.
40. Chan C, Saad A, Randleman JB, et al. Analysis of cases and accuracy of 3 risk scoring systems in predicting ectasia after laser in situ keratomileusis. J Cataract Refract Surg. 2018;44:979–92.
41. Demir S, Sönmez B, Yeter V, Ortak H. Comparison of normal and keratoconic corneas by Galilei dual-Scheimpflug analyzer. Contact Lens Anter Eye. 2013;36:219–25.
42. Smadja D, Touboul D, Cohen A, et al. Detection of subclinical keratoconus using an automated decision tree classification. Am J Ophthalmol. 2013;156:237–46.e1.

43. Jafarinasab MR, Feizi S, Karimian F, Hasanpour H. Evaluation of corneal elevation in eyes with subclinical keratoconus and keratoconus using Galilei double Scheimpflug analyzer. Eur J Ophthalmol. 2013;23:377–84.
44. Ambrósio R Jr, Nogueira LP, Caldas DL, et al. Evaluation of corneal shape and biomechanics before LASIK. Int Ophthalmol Clin. 2011;51:11–38.
45. Lopes BT, Ramos IC, Dawson DG, Belin MW, Ambrósio R Jr. Detection of ectatic corneal diseases based on Pentacam. Z Med Phys. 2016;26:136–42.
46. Ambrósio R Jr, Dawson DG, Salomao M, Guerra FP, Caiado AL, Belin MW. Corneal ectasia after LASIK despite low preoperative risk: tomographic and biomechanical findings in the unoperated, stable, fellow eye. J Refract Surg. 2010;26:906–11.
47. Ambrósio R Jr, Belin M. Enhanced screening for ectasia risk prior to laser laser vision correction. Int J Keratoconus Ectatic Corneal Dis. 2017;6:23–33.
48. Lopes BT, Ramos IC, Salomao MQ, et al. Enhanced tomographic assessment to detect corneal ectasia based on artificial intelligence. Am J Ophthalmol. 2018;195:223–32.
49. Ambrósio R Jr, Ramos I, Lopes B, et al. Assessing ectasia susceptibility prior to LASIK: the role of age and residual stromal bed (RSB) in conjunction to Belin–Ambrósio deviation index (BAD-D). Rev Bras Oftalmol. 2014;73:75–80.
50. Reinstein DZ, Silverman RH, Rondeau MJ, Coleman DJ. Epithelial and corneal thickness measurements by high-frequency ultrasound digital signal processing. Ophthalmology. 1994;101:140–6.
51. Salomao MQ, Hofling-Lima AL, Lopes BT, et al. Role of the corneal epithelium measurements in keratorefractive surgery. Curr Opin Ophthalmol. 2017;28:326–36.
52. Reinstein DZ, Gobbe M, Archer TJ, Silverman RH, Coleman DJ. Epithelial, stromal, and total corneal thickness in keratoconus: three-dimensional display with Artemis very-high frequency digital ultrasound. J Refract Surg. 2010;26:259–71.
53. Reinstein DZ, Archer TJ, Urs R, Gobbe M, RoyChoudhury A, Silverman RH. Detection of keratoconus in clinically and algorithmically topographically normal fellow eyes using epithelial thickness analysis. J Refract Surg. 2015;31:736–44.
54. Li Y, Chamberlain W, Tan O, Brass R, Weiss JL, Huang D. Subclinical keratoconus detection by pattern analysis of corneal and epithelial thickness maps with optical coherence tomography. J Cataract Refract Surg. 2016;42:284–95.
55. Li Y, Tan O, Brass R, Weiss JL, Huang D. Corneal epithelial thickness mapping by Fourier-domain optical coherence tomography in normal and keratoconic eyes. Ophthalmology. 2012;119:2425–33.
56. Pahuja N, Shroff R, Pahanpate P, et al. Application of high resolution OCT to evaluate irregularity of Bowman's layer in asymmetric keratoconus. J Biophotonics. 2017;10:701–7.
57. Gomes JA, Tan D, Rapuano CJ, et al. Global consensus on keratoconus and ectatic diseases. Cornea. 2015;34:359–69.
58. Luce DA. Determining in vivo biomechanical properties of the cornea with an ocular response analyzer. J Cataract Refract Surg. 2005;31:156–62.
59. Fontes BM, Ambrósio Junior R, Jardim D, Velarde GC, Nose W. Ability of corneal biomechanical metrics and anterior segment data in the differentiation of keratoconus and healthy corneas. Arq Bras Oftalmol. 2010;73:333–7.
60. Luz A, Fontes BM, Lopes B, Ramos I, Schor P, Ambrósio R Jr. ORA waveform–derived biomechanical parameters to distinguish normal from keratoconic eyes. Arq Bras Oftalmol. 2013;76:111–7.
61. Luz A, Lopes B, Hallahan KM, et al. Discriminant value of custom ocular response analyzer waveform derivatives in forme fruste keratoconus. Am J Ophthalmol. 2016;164:14–21.
62. Hallahan KM, Sinha Roy A, Ambrósio R Jr, Salomao M, Dupps WJ Jr. Discriminant value of custom ocular response analyzer waveform derivatives in keratoconus. Ophthalmology. 2014;121:459–68.
63. Luz A, Lopes B, Hallahan KM, et al. Enhanced combined tomography and biomechanics data for distinguishing forme fruste keratoconus. J Refract Surg. 2016;32:479–94.

64. Ambrósio R Jr, Ramos I, Luz A, et al. Dynamic ultra high speed Scheimpflug imaging for assessing corneal biomechanical properties. Rev Bras Oftalmol. 2013;72:99–102.
65. Salomao MQ, Hofling-Lima AL, Faria-Correia F, et al. Dynamic corneal deformation response and integrated corneal tomography. Indian J Ophthalmol. 2018;66:373–82.
66. Ali NQ, Patel DV, McGhee CN. Biomechanical responses of healthy and keratoconic corneas measured using a noncontact Scheimpflug-based tonometer. Invest Ophthalmol Vis Sci. 2014;55:3651–9.
67. Steinberg J, Katz T, Lucke K, Frings A, Druchkiv V, Linke SJ. Screening for keratoconus with new dynamic biomechanical in vivo Scheimpflug analyses. Cornea. 2015;34:1404–12.
68. Vinciguerra R, Ambrósio R Jr, Elsheikh A, et al. Detection of keratoconus with a new biomechanical index. J Refract Surg. 2016;32:803–10.
69. Sedaghat MR, Momeni-Moghaddam H, Ambrósio R Jr, et al. Diagnostic ability of corneal shape and biomechanical parameters for detecting frank keratoconus. Cornea. 2018;37:1025–34.
70. Manche E, Roe J. Recent advances in wavefront-guided LASIK. Curr Opin Ophthalmol. 2018;29:286–91.
71. Colak HN, Kantarci FA, Yildirim A, et al. Comparison of corneal topographic measurements and high order aberrations in keratoconus and normal eyes. Contact Lens Anter Eye. 2016;39:380–4.
72. Jafri B, Li X, Yang H, Rabinowitz YS. Higher order wavefront aberrations and topography in early and suspected keratoconus. J Refract Surg. 2007;23:774–81.
73. Schlegel Z, Lteif Y, Bains HS, Gatinel D. Total, corneal, and internal ocular optical aberrations in patients with keratoconus. J Refract Surg. 2009;25:S951–7.
74. Naderan M, Jahanrad A, Farjadnia M. Ocular, corneal, and internal aberrations in eyes with keratoconus, forme fruste keratoconus, and healthy eyes. Int Ophthalmol. 2018;38:1565–73.
75. Saad A, Gatinel D. Evaluation of total and corneal wavefront high order aberrations for the detection of forme fruste keratoconus. Invest Ophthalmol Vis Sci. 2012;53:2978–92.
76. Imbornoni LM, Padmanabhan P, Belin MW, Deepa M. Long-term tomographic evaluation of unilateral keratoconus. Cornea. 2017;36(11):1316–24.
77. Ramos I, Reinstein DZ, Archer T. Unilateral ectasia characterized by advanced diagnostic tests. Int J Keratoconus Ectatic Corneal Dis. 2016;5:40–51.
78. Henriquez MA, Hadid M, Izquierdo L Jr. A systematic review of subclinical keratoconus and forme fruste keratoconus. J Refract Surg. 2020;36:270–9.